AAS 05-112

Venus and Mars Gravity-Assist Trajectories to Jupiter Using Nuclear Electric Propulsion

Daniel W. Parcher* **and Jon A. Sims**ϒ

Optimal low-thrust gravity-assist trajectories to Jupiter using nuclear electric propulsion are presented. Venus, double Venus, and Mars gravity-assist cases are examined. For each of these cases, two locally optimal trajectory categories, differentiated by number of heliocentric revolutions, are considered. The solutions that use fewer heliocentric revolutions perform better at short flight times, but do not perform as well at long flight times. Of the gravity-assist types examined, the Mars gravity-assist offers the most delivered mass to Jupiter for most flight times.

INTRODUCTION

For interplanetary missions, highly efficient electric propulsion systems can be used to increase the mass delivered to the destination and/or reduce the trip time over typical chemical propulsion systems.[1, 2] This technology has been demonstrated on the Deep Space 1 mission [3] – part of NASA's New Millennium Program to validate technologies which can lower the cost and risk and enhance the performance of future missions. With the successful demonstration on Deep Space 1, future missions can consider electric propulsion as a viable propulsion option.

Another proven technique for enhancing the performance of an interplanetary mission is the use of planetary gravity assists, as exemplified by the Voyager, Galileo, and Cassini missions. Flying a spacecraft with an electric propulsion system on a gravity-assist trajectory can enable missions that would otherwise be impractical to execute.

NASA's Prometheus program is developing nuclear power and high power electric propulsion capabilities for deep space missions. Missions like the Jupiter Icy Moons Orbiter, proposed as the first mission of the Prometheus program, are the motivation behind the work presented here. The propulsion system characteristics chosen for this study may be similar to those used by Prometheus missions.

In this paper, we present trajectories that rendezvous with Jupiter using nuclear electric propulsion and gravity assists with Venus or Mars and compare them to direct trajectories (i.e., no gravity assists). We also present and describe a variety of locally optimal trajectories for each of the following gravity assist types: single Venus gravity assist, double Venus gravity assist, and Mars gravity assist.

Other researchers have presented gravity-assist trajectories to Jupiter using solar electric propulsion.[4, 5] However, these trajectories do not rendezvous (i.e., reduce the hyperbolic excess velocity to zero) with Jupiter using electric propulsion due to the fact that the solar power system is ineffective at such large distances from the Sun. By using a nuclear power source, the thrust capability of the electric

* Member of the Engineering Staff, Outer Planet/Small Body Flight Dynamics Section, Jet Propulsion Laboratory, California Institute of Technology, Mail Stop 301-140L, 4800 Oak Grove Drive, Pasadena, California 91109-8099. E-mail: Daniel.W.Parcher@jpl.nasa.gov. Phone: (818) 393-0457, Fax: (818) 393-6388.

ϒ Technical Manager, Outer Planet/Small Body Flight Dynamics Section, Jet Propulsion Laboratory, California Institute of Technology, Mail Stop 301-140L, 4800 Oak Grove Drive, Pasadena, California 91109-8099. E-mail: Jon.A.Sims@jpl.nasa.gov. Phone: (818) 354-0313, Fax: (818) 393-6388.

propulsion system does not diminish with distance from the Sun; hence, it can be used to accomplish the rendezvous with Jupiter. A few gravity-assist trajectories to Jupiter using nuclear electric propulsion have also been presented by others, including a Mars gravity assist case. [6]

In future papers we plan to present similar types of results for nuclear electric propulsion trajectories to Jupiter using Earth gravity assists and Venus and Earth gravity assists.

APPROACH

The preliminary design software used in this study to discover and analyze the trajectories is based on the technique presented by Sims and Flanagan.[7] It uses a direct optimization method and models the thrust as small impulses. The starting and ending bodies (Earth and Jupiter, in this case) are treated as massless. The gravity assists are modeled as instantaneous changes in the direction of the $\mathbf{V}_\infty$ (hyperbolic relative velocity vector).

The maximum power available to the propulsion system is assumed fixed at 95 kW. The thrusters are modeled with a specific impulse of 6000 s and an efficiency of 70%. These parameters yield a maximum thrust of 2.26 N with a mass flow rate of 3.84×10^{-5} kg/s. The software can choose whether or not to thrust at any point in time, the level of the thrust up to the maximum, and the direction of thrust.

The trajectories presented are injected to a positive energy with respect to Earth. The launch vehicle used for these trajectories has three times the capability of the Delta IV Heavy. The performance curve for this launch vehicle is illustrated in Figure 1 which shows the relationship between injection C_3 (defined as the square of V_∞ vector magnitude) and injected mass. In each of the trajectories presented, the injection V_∞ will be optimized in both direction and magnitude in order to maximize the final mass at Jupiter.

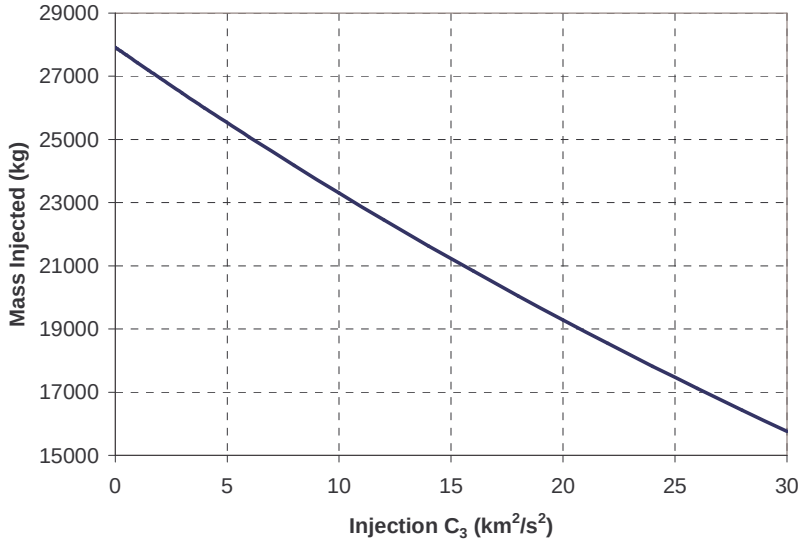

Figure 1 Launch Vehicle Capability Model

The performance curve in Figure 1 shows that injected mass is reduced substantially as the injection C_3 is increased. This relationship effectively penalizes trajectories that require higher injection C_3 values and provides the optimizer with an incentive to reduce C_3.

DIRECT TRANSFERS

The first trajectories presented here are direct transfers to Jupiter. These trajectories will serve as a baseline for comparison with the different gravity assist combinations. For a given time of flight, there can be several locally optimal solutions for an Earth to Jupiter transfer distinguished by the number of

heliocentric revolutions. The number of revolutions for the globally optimal solution depends on the flight time, propulsion capability, and launch vehicle capability. Specifying a time of flight will put a lower and upper bound on the number of heliocentric revolutions that can be attained with the propulsion system and greatly reduce the number of trajectory families to be considered.

>2 Heliocentric Revolution Family

Figure 2 is an example of a locally optimal low-thrust trajectory starting with a positive C_3 injection at Earth and ending at Jupiter capture with no intermediate flybys. The optimized injection C_3 for the trajectory in Figure 2 is 0.64 km^2/s^2 and the flight time is constrained to be less than or equal to 7.5 years. In this case, the optimal result uses the entire 7.5 years to accomplish the transfer. This solution arrives at Jupiter after more than 2 heliocentric revolutions and has one large coast arc (represented by the lack of arrows) on the final revolution. At higher flight times, additional coast arcs will begin to appear as thrusting shifts to the most effective places in the transfer. At flight times below 7.5 years, the coast arc present in this trajectory will begin to close, replaced by more thrusting. As flight time is reduced, the performance for this solution will begin to fall off quickly as more and more thrusting occurs at less effective places in the transfer. If the reduction in flight time is sufficiently large, the coast arc will close and the all-propulsive limit for this trajectory type will be achieved.

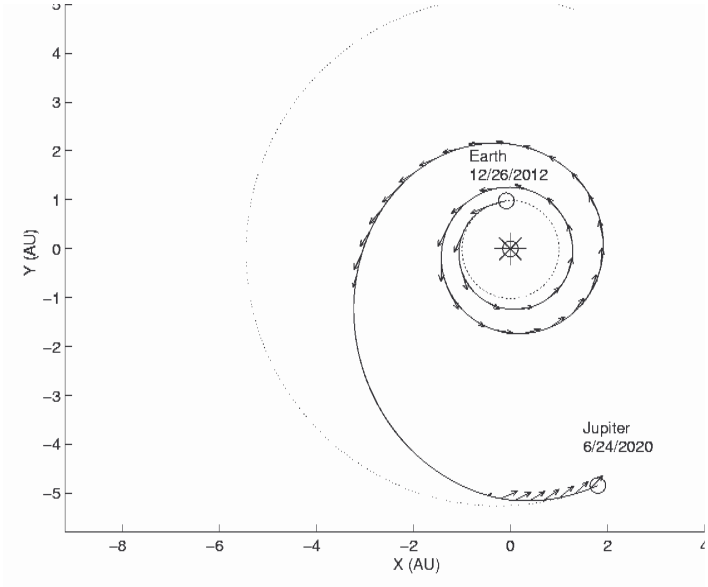

Figure 2 Direct Earth to Jupiter Transfer, 7.5 yr. Time of Flight, >2 Heliocentric Revolutions[1]

Figure 3 shows the evolution of semimajor axis and eccentricity for the transfer in Figure 2. The chart shows that the transfer is accomplished with a gradual increase in aphelion and eccentricity until the trajectory reaches a transfer orbit that will take the spacecraft to Jupiter. As the spacecraft approaches rendezvous, thrusting occurs to circularize the trajectory. Circularization is indicated with a decrease in eccentricity and an increase in perihelion.

[1] The thrust vectors plotted along the trajectories presented may have different densities on different legs (defined to be between body encounters) of a trajectory. However, the density will not vary within a given leg. The variation in density from one leg to the next is for fidelity purposes and to ensure that thrust direction is discernable. In these graphics, thrusting occurs constantly where arcs of thrust vectors are present.

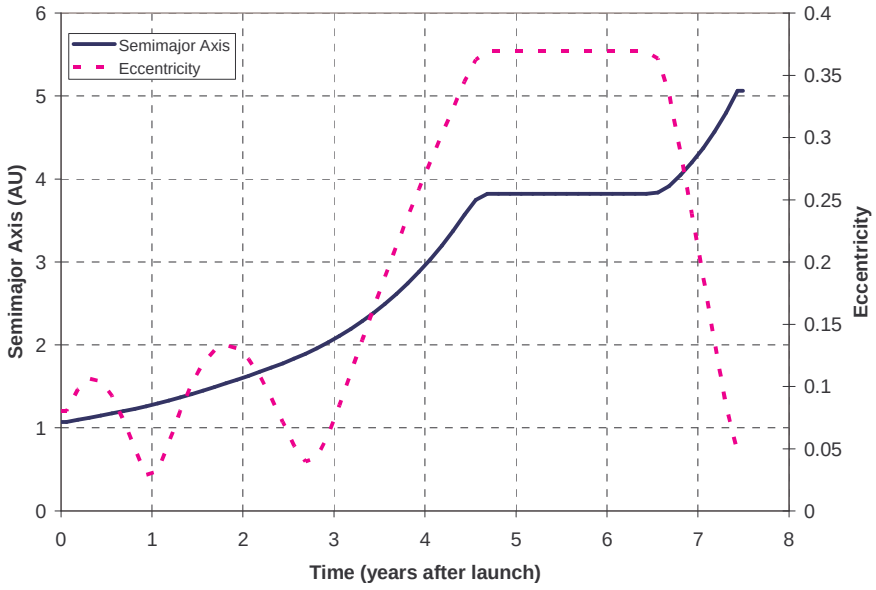

Figure 3 Direct Earth to Jupiter Transfer, >2 Heliocentric Revolutions - Evolution of Semimajor Axis and Eccentricity

>1 Heliocentric Revolution Family

The geometry of the trajectory in Figure 2 causes it to underperform other locally optimal trajectories at some flight times. At lower flight times, trajectories that have fewer heliocentric revolutions deliver more mass. Figure 4 is an example of a trajectory with fewer heliocentric revolutions optimized for a 6 year flight time with an optimal injection C_3 of 6.76 km^2/s^2. The trajectory shown in Figure 4 belongs to the family of trajectories that, at this flight time, has more than 1 but less than 2 heliocentric revolutions. Figures 2 and 4 represent two different locally optimal trajectory families that both accomplish the Earth-to-Jupiter transfer.

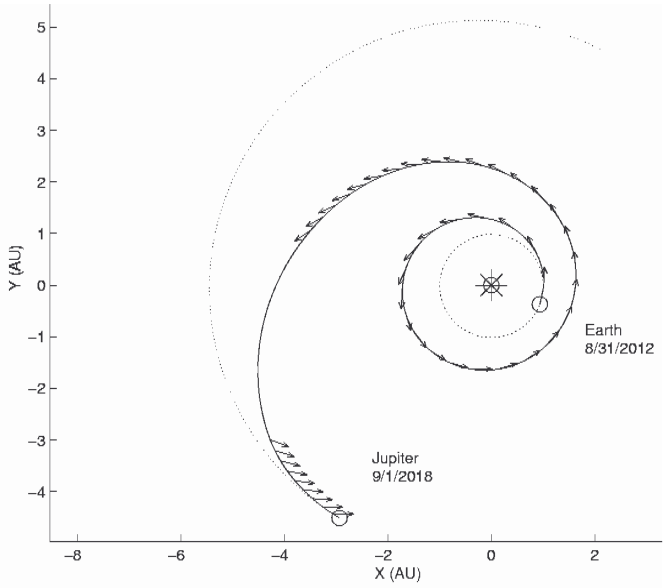

Figure 4 Direct Earth to Jupiter Transfer, 6 yr. Time of Flight, >1 Heliocentric Revolution

Much like the trajectory shown in Figure 2, this trajectory has only one coast arc. However, this trajectory uses a significantly larger injection C_3 from the launch vehicle, enabling it to accomplish the same transfer with fewer heliocentric revolutions. In general, the optimal injection C_3 will increase as either heliocentric revolutions or flight time is decreased.

Performance Comparison

Trajectories with larger numbers of revolutions generally perform better at longer flight times due to a decreased initial C_3 (and corresponding increased initial mass) and the ability to have more efficient thrust arcs. Optimal low-thrust circle to circle rendezvous trajectories that have many heliocentric revolutions begin to approximate Hohmann transfers both in the positioning of thrust arcs and in total ΔV [8]. Such a trajectory will thrust at perihelion for short periods of time, waiting until the next revolution to continue raising aphelion rather than thrust at an inefficient time. Once aphelion is near the target, short thrust arcs will occur at aphelion to raise perihelion until rendezvous is achieved. In this manner, trajectories with many revolutions are able to have very efficient thrust profiles and can deliver more mass to the target than trajectories with fewer revolutions (assuming flight time is free).

Additional heliocentric revolutions may allow for more efficient thrust arcs, but they cause performance to fall off quickly as time of flight is decreased. The delivered mass as a function of flight time for the solution families shown in Figures 2 and 4 is presented in Figure 5[2].

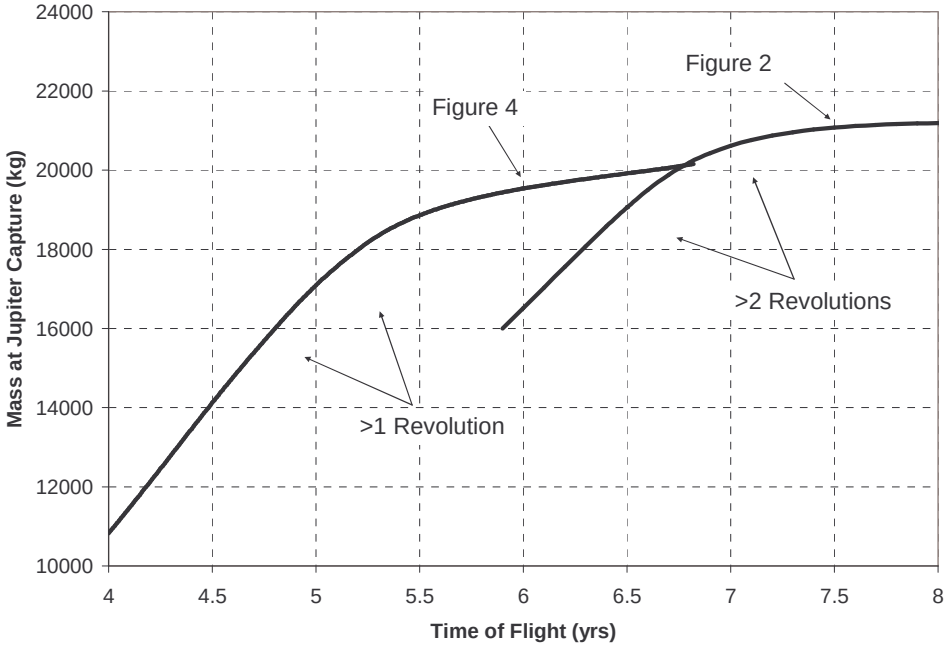

Figure 5 Direct Earth to Jupiter Transfers – Delivered Mass vs. Time of Flight

The curve in Figure 5 that extends to lower times of flight is a family of solutions that circle the Sun more than once but less than twice (Figure 4). The curve that extends to the higher flight times is the family of solutions with an additional revolution, illustrated in Figure 2. Note that at the point where these

[2] The time of flight trades shown in Figures 5 and 6 were generated for the same set of direct transfers using different software than that used to generate Figures 2 and 4. The trades in Figures 5 and 6 differ from others presented in this paper in that they were generated using circular, coplanar orbits of Earth and Jupiter. This was done to allow the direct transfer results to be general in terms of launch opportunity. The circular, coplanar simplifying assumption was not used for the gravity-assist results since performance can depend significantly on injection opportunity.

two curves intersect, two low-thrust trajectories with very different geometries accomplish the Earth to Jupiter transfer with the same flight time and the same delivered mass. This highlights the need to seek out several locally optimal solutions when examining time of flight trades. It is also important to note that the trajectory with the higher number of revolutions offers only a limited amount of increased mass, while the other solution offers a substantial reduction in flight time. A locally optimal solution that requires less than one heliocentric revolution to rendezvous with Jupiter exists for this problem; however, this solution does not deliver the most mass until the flight time is below 4 years. Similarly, a solution with more than 3 heliocentric revolutions exists, but the flight time is longer than we wish to consider here.

Figure 6 illustrates how the optimal injection C_3 varies with flight time for the different solutions. Notice that the >2 revolution trajectory has substantially lower C_3 values at flight times greater than 6.5 years. The variation in launch vehicle performance with C_3 has a strong effect on delivered mass.

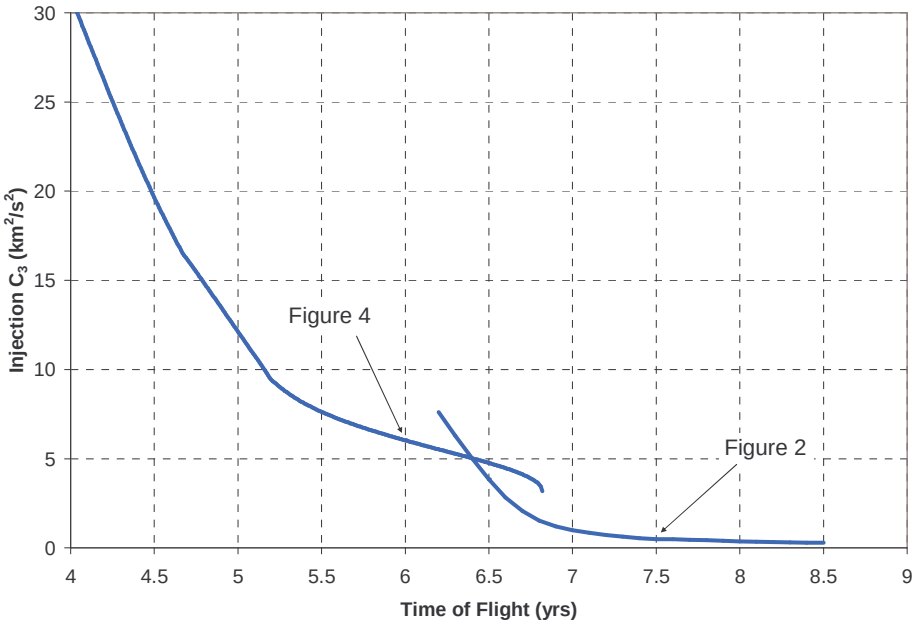

Figure 6 Direct Earth to Jupiter Transfers - Injection C_3 vs. Flight Time

The issue of locally optimal solutions can become more complex when planetary flybys are included because at least one locally optimal solution could exist for each number of heliocentric revolutions between each set of encounters.

SINGLE VENUS GRAVITY ASSIST

The single Venus gravity-assist (VGA) trajectories presented in this paper inject in the general direction of Earth's orbit such that they pass through an aphelion substantially beyond 1 AU prior to encountering Venus. Trajectories that inject inward toward Venus and use a single Venus flyby as the only gravity assist are very poor performing, so they are not included. We present two locally optimal solutions differentiated by number of heliocentric revolutions prior to encountering Venus.

Type 2-3

The first type of solution has approximately one revolution prior to the Venus flyby. This family will be referred to as a Type 2-3 VGA since the transfer from Earth to Venus is Type 2 (more than 180^o but less than 360^o about the Sun) for some launch opportunities and flyby conditions, and Type 3 (more than 360^o but less than 540^o about the Sun) for others. A plot of this trajectory is shown in Figure 7. The flight time for the trajectory in Figure 7 is 5 years with a corresponding optimal injection C_3 of 9.9 km^2/s^2.

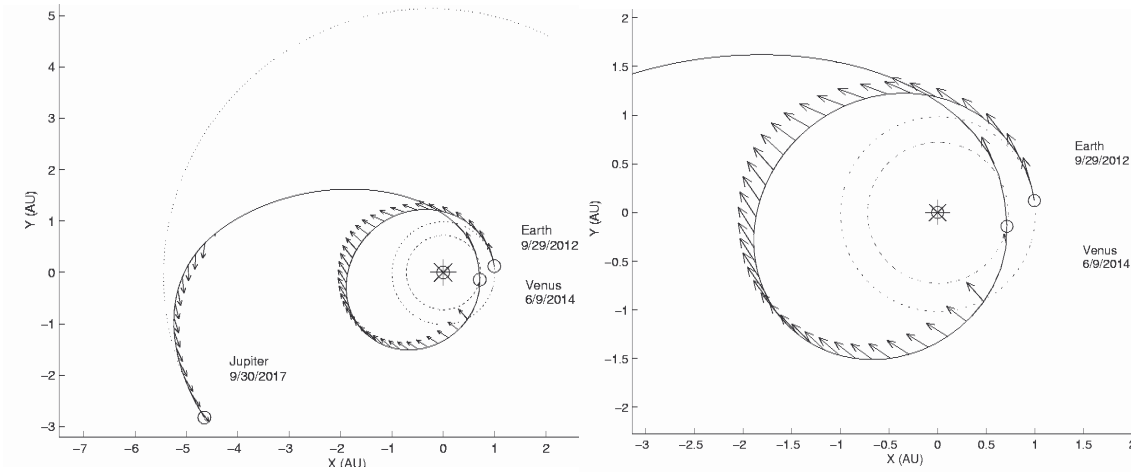

Figure 7 Venus Gravity Assist to Jupiter – Approximately 1 Heliocentric Revolution to Venus (Type 2-3)

Type 4-5

The second type of Venus gravity assist, shown in Figure 8, has almost two heliocentric revolutions before the first Venus encounter. This family will be referred to as a Type 4-5 VGA since the Earth to Venus transfer is Type 4 (more than 540° but less than 720°) for some injection opportunities and flight times and a Type 5 (more than 720° but less than 900°) for others. Both the Type 2-3 and the Type 4-5 VGA trajectories, much like the direct (no gravity assist) trajectories, use the low-thrust propulsion system immediately after injection to augment the injection V_∞, keeping the energy supplied by the launch vehicle low. The VGA trajectory shown in Figure 8 has a higher time of flight than the Type 2-3, but it has a lower injection C_3, allowing more of the ΔV for the mission to be performed by the efficient ion engines. Here, the initial C_3 is only 1.96 km^2/s^2 for a time of flight of 6 years. The flyby altitude at Venus was constrained to be no less than 200 km for both VGA cases.

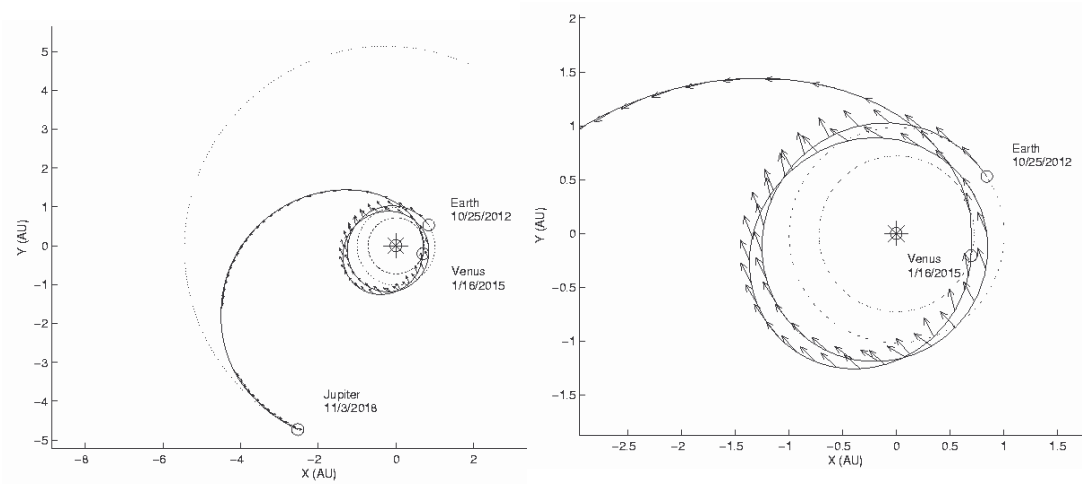

Figure 8 Venus Gravity Assist to Jupiter – Approximately 2 Heliocentric Revolutions to Venus (Type 4-5)

Subcategories of Local Optima

Even within the Type 2-3 and Type 4-5 VGA categories there are other locally optimal solutions distinguishable by the Earth-Venus transfer time. These local minima will reach Venus an integer multiple of Venus years earlier or later. To achieve a longer flight time to Venus with the same number of revolutions, a larger injection C_3 may be required to achieve the larger aphelion. If the time of flight to Venus is too short, then the V_∞ at Venus may not be sufficient to accomplish the transfer to Jupiter. The result is a trade between injection C_3 and Venus flyby V_∞ across locally optimal solutions to determine which Earth-Venus transfer time is best for that number of heliocentric revolutions.

Another distinguishing characteristic between local optima for the VGA cases is the type of Venus flyby. The VGA types shown in Figures 7 and 8 both have Venus flybys that occur as the distance between the spacecraft and Sun is decreasing (inbound). Other transfer families exist that have Venus flybys such that the distance between the spacecraft and Sun is increasing (outbound). Figure 9 shows an example of a Type 2-3 VGA with an outbound Venus flyby for a launch date in 2014. An outbound VGA case also exists for the 2012 launch date. However, that opportunity is not phased well enough with Jupiter to deliver reasonable mass, so the 2014 opportunity is used to illustrate this trajectory type.

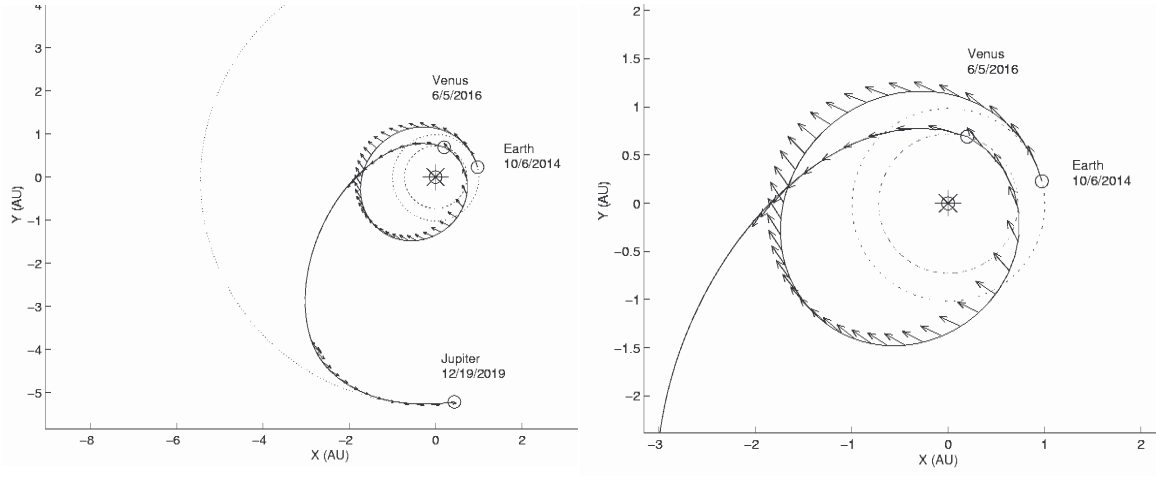

Figure 9 Venus Gravity Assist to Jupiter – Type 2-3 Transfer to Venus, Outbound Venus Flyby

Performance Comparison

Figure 10 illustrates the trade space of time of flight and mass delivered to Jupiter for the two types of inbound Venus gravity-assist trajectories shown and demonstrates that the Type 4-5 VGA performs poorly at low times of flight, but offers more delivered mass at longer flight times. Looking at the knees of these curves indicates that for an additional year of flight time, the Type 4-5 solution offers an additional 2000 kg (approximately 10%) to Jupiter. The performance curves for the direct transfers (Figure 5) are included in Figure 10 for comparison.

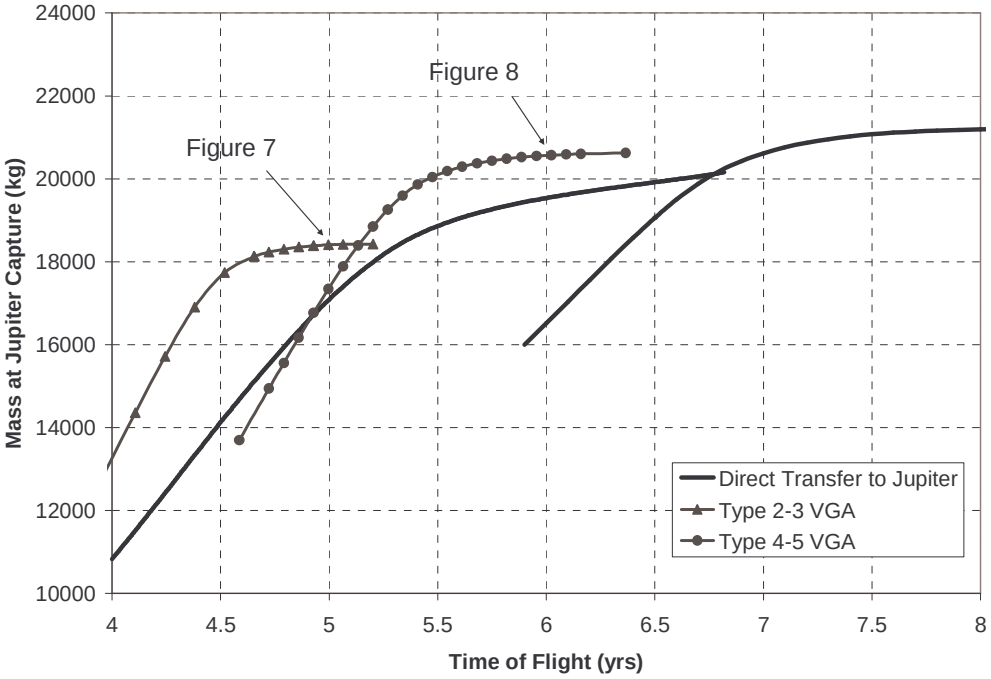

Figure 10 Venus Gravity Assists to Jupiter – Delivered Mass vs. Time of Flight

As with the direct trajectories, there is a point at which these two curves cross, indicating that there exists one time of flight at which these two geometrically distinct trajectory types deliver the same mass to Jupiter. The single Venus gravity-assist cases outperform the direct cases at most flight times. Both VGA types occur roughly each year with significant performance differences from one opportunity to the next.

DOUBLE VENUS GRAVITY ASSIST

As with the single Venus gravity assist, there are two main types of double Venus gravity-assist (VVGA) trajectories presented here. The first category is the shorter time of flight solution illustrated in Figure 11. The trajectory in Figure 11 has a Type 1 transfer (<180^o about the Sun) to Venus, but this category will be referred to as a Type 1-2 VVGA since different launch years and flight times can result in either Type 1 or Type 2 transfers to the first Venus flyby. The second category is a longer flight time solution illustrated in Figure 12. The trajectory in Figure 12 uses a Type 4 trajectory from Earth to Venus. This category of VVGA will be referred to as Type 3-4 since different injection opportunities or flight times can result in either a Type 3 or 4 transfer to Venus. Again, the flyby altitude at Venus was constrained to be greater than 200 km.

Type 1-2

The Type 1-2 VVGA in Figure 11 has a 5 year time of flight with an optimal injection C_3 of 7.84 km^2/s^2. After the Venus flyby, V_∞ leveraging occurs (thrusting at aphelion to reduce perihelion below Venus's orbit radius), improving the effectiveness of the second Venus flyby [9]. Notice that the second Venus flyby is an outbound encounter; another VVGA trajectory exists with an inbound flyby at the second Venus encounter.

The trajectory in Figure 11 returns to Venus approximately 2 Venus years after the first flyby. As with the VGA cases, other local optima exist with different numbers of Venus years between encounters.

However, the lack of thrusting immediately following the flybys indicates that a larger flight time between Venus encounters would likely not offer more delivered mass.

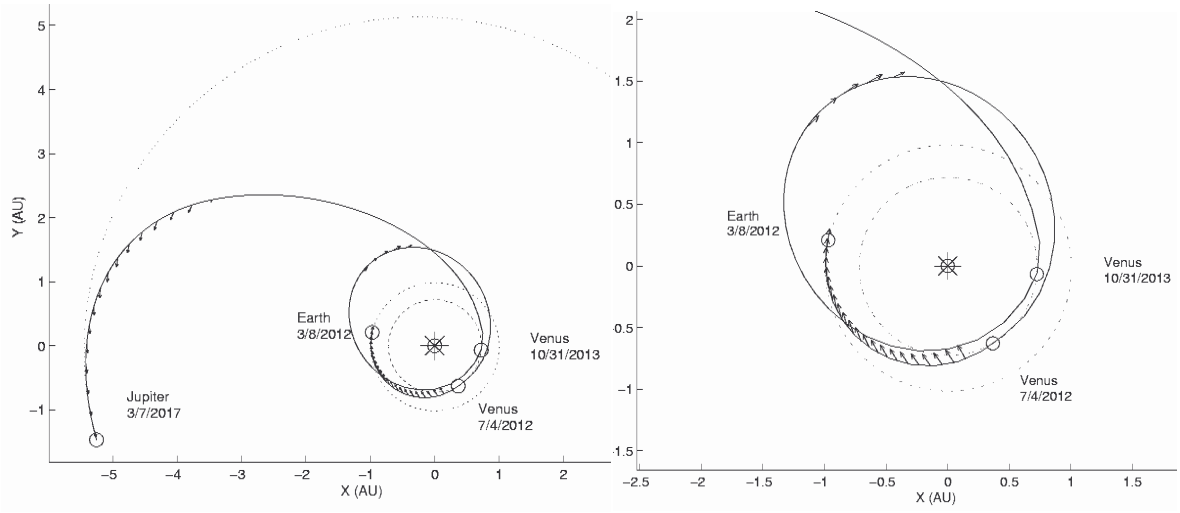

Figure 11 Double Venus Gravity Assist to Jupiter – Less than 1 Heliocentric Revolution to the First Venus Flyby (Type 1-2)

Type 3-4

Figure 12 shows a Type 3-4 VVGA. Again, thrusting for V_∞ levaraging occurs at aphelion of the Venus-Venus transfer. The trajectory plotted in Figure 12 has a flight time of approximately 6 years, a injection C_3 of 4.41 km^2/s^2, and takes slightly less than 2 Venus years to accomplish the Venus-to-Venus transfer. The additional heliocentric revolution prior to the first flyby enables this trajectory type to use less initial C_3 than the Type 1-2 VVGA.

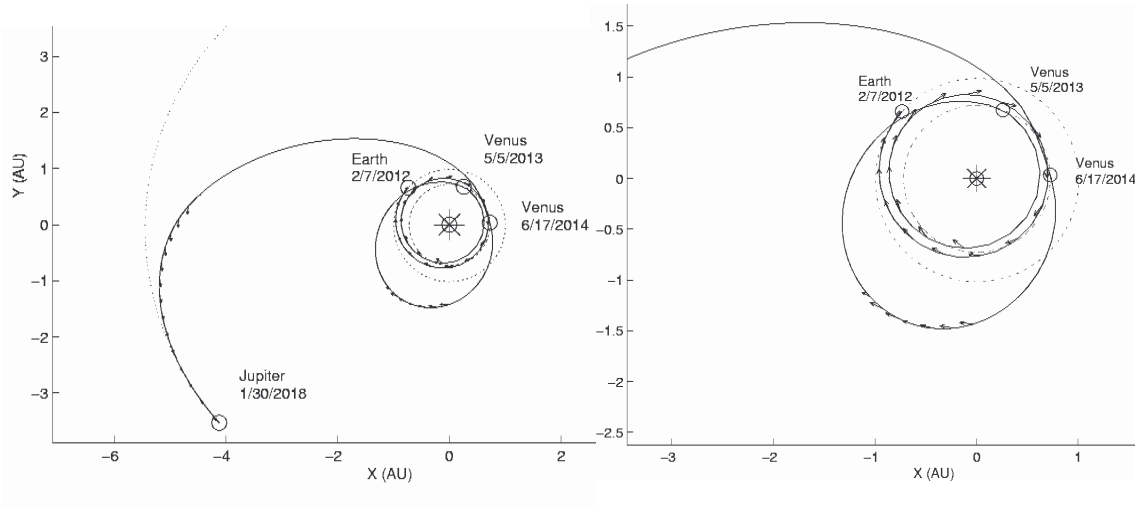

Figure 12 Double Venus Gravity Assist to Jupiter – Less than 2 Heliocentric Revolutions to the First Venus Flyby (Type 3-4)

In Figure 12, the second Venus encounter occurs inbound. Another locally optimal Type 3-4 VVGA that has an outbound flyby at the second Venus encounter can exist. Many other locally optimal types of VVGAs exist.

The correct Earth-Venus phasing for the VVGA occurs every synodic period (1.5 years). However, roughly speaking, every other Earth-Venus opportunity will have Venus on the wrong side of the solar system for an efficient transfer to Jupiter. Thus favorable phasing for the Type 1-2 VVGA only occurs every 3 years with minor differences in performance between opportunities. On the other hand, favorable phasing for the Venus-Jupiter transfer occurs every year. So opportunities for the Type 3-4 VVGA occur most years with larger variations in performance between opportunities.

Performance Comparison

It is interesting to note that the Type 3-4 VVGA in Figure 12 burns more than 3 times as much propellant before the first Venus flyby as the Type 1-2. However, due to the lower injection C_3 and correspondingly greater injected mass, the mass delivered to the first Venus flyby by the Type 3-4 case is substantially higher. In fact, the Type 3-4 VVGA uses more total ΔV but delivers more mass to Jupiter at high flight times.

The trade between time of flight and delivered mass is illustrated in Figure 13. Again, taking points from the knees of the curves for the two types of solutions, the Type 3-4 VVGA offers 600 kg (just under 3%) of additional mass delivered to Jupiter at the cost of almost one year of flight time.

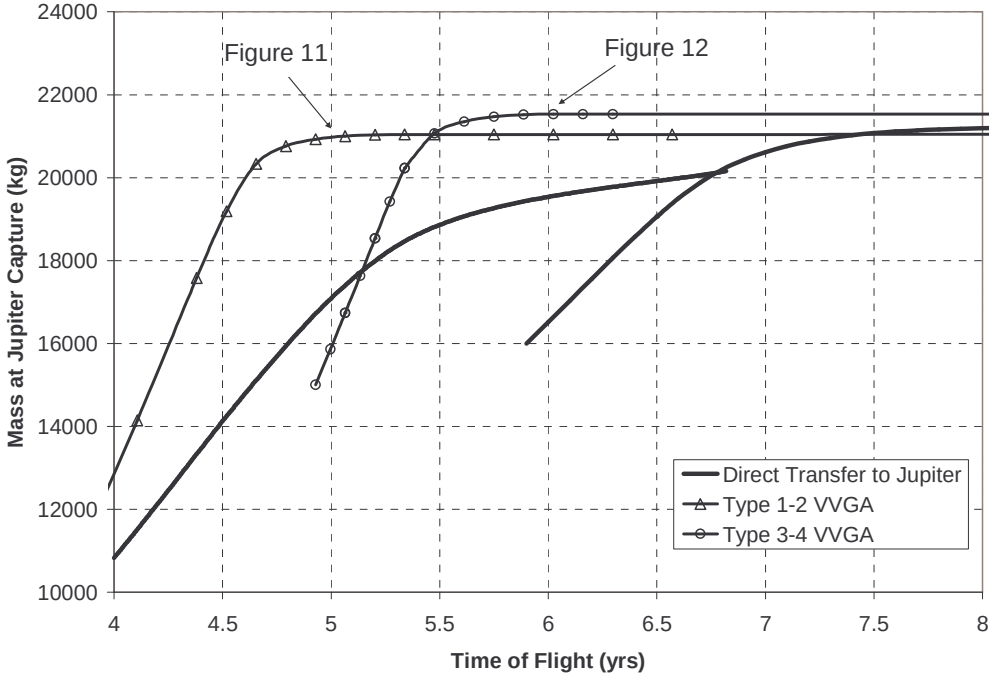

Figure 13 Double Venus Gravity Assists to Jupiter - Delivered Mass vs. Time of Flight

A comparison between Figures 10 and 13 shows that at most fight times, the double Venus gravity assist performs better than the single Venus gravity assist. This result is expected as this option gets the benefit of a second Venus flyby. However, it is interesting to note that the VVGA cases underperform the Type 2-3 VGA at very low times of flight.

MARS GRAVITY ASSIST

As with the previous gravity assist cases, there are two main types of Mars gravity assist (MGA) trajectories presented here. The first family uses less than 1 heliocentric revolution to the Mars flyby and will be referred to as a Type 1-2 MGA. The second family uses greater than 1 heliocentric revolution to the Mars flyby and will be referred to as a Type 3-4 MGA. The flyby altitude at Mars is constrained to be no less than 600 km. Studies on the effect of the minimum flyby altitude constraint have shown low performance sensitivity to small changes in the minimum flyby altitude for the Mars cases.

Type 1-2

The Type 1-2 MGA is shown in Figure 14. As with the previous gravity-assist cases, this trajectory requires greater injection C_3 than its multi-rev counterpart. The trajectory in Figure 14 has a time of flight of approximately 6 years with an optimal injection C_3 of 2.89 km^2/s^2. Mars is less massive than Venus, further from the sun, and, due to its larger orbital period, is less often phased properly with Jupiter. However, since the C_3 required for this trajectory is substantially lower than the injection C_3 values for the multiple-revolution-to-Venus VGAs and VVGAs, one might expect the Mars case to perform well in comparison.

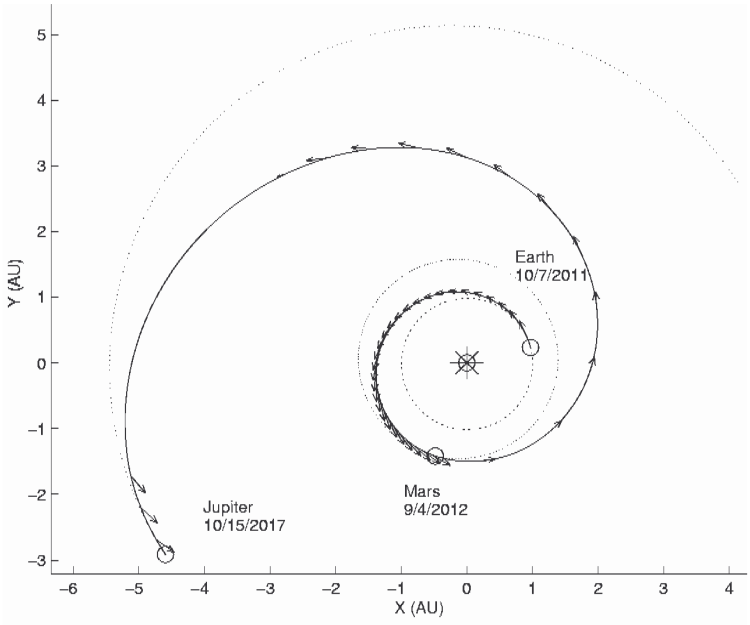

Figure 14 Mars Gravity Assist to Jupiter – Less Than 1 Heliocentric Revolution to Mars (Type 1-2)

Type 3-4

The other type of Mars gravity-assist trajectory presented travels more than 1 heliocentric revolution before encountering Mars. Figure 15 shows the Type 3-4 MGA optimized for a 6 year trajectory flight time. The trajectory in Figure 15 has an optimal injection C_3 of 1.69 km^2/s^2, substantially less than any of the other gravity-assist trajectories discussed here. This trajectory, as with the Type 1-2 MGA, augments the injection V_∞ with an initial thrust arc immediately after injection in an attempt to reduce the C_3 supplied by the launch vehicle as much as possible while satisfying the flight time constraints and meeting the optimal phasing for the gravity assist. Here again the total propellant consumption for the multiple revolution case is greater than for the Type 1-2 case. Again, the difference in injected mass is greater than the difference in propellant consumption resulting in a larger mass delivered to Jupiter by the Type 3-4 MGA.

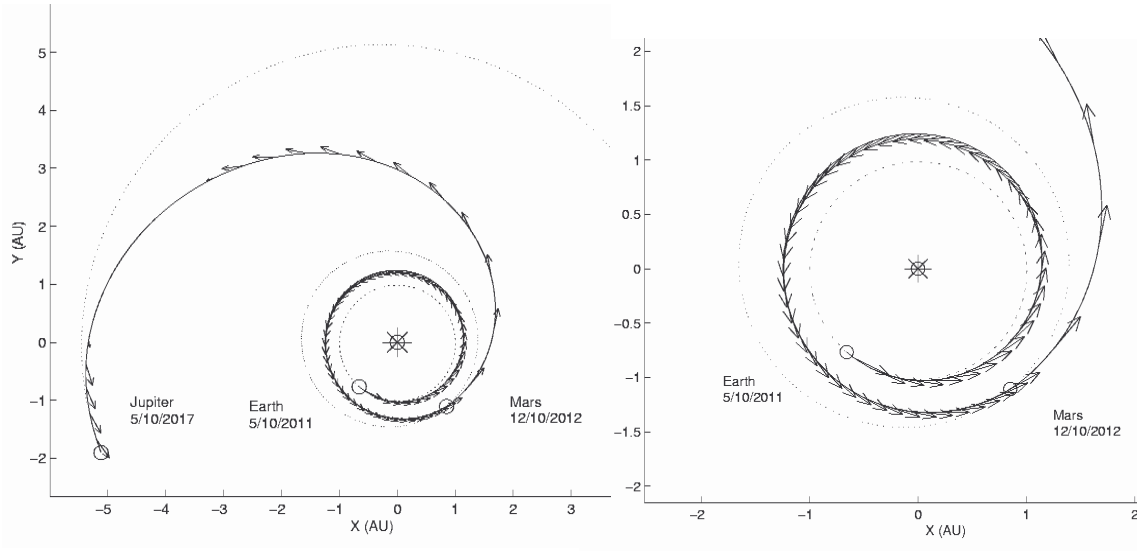

Figure 15 Mars Gravity Assist to Jupiter – Greater than 1 Heliocentric Revolution to Mars (Type 3-4)

Performance Comparison

The trade between time of flight and delivered mass for the Mars gravity-assist types are illustrated in Figure 16. The performance of the two types of Mars gravity assists does not differ as much as the other cases. This result is due to the fact that the difference in initial C_3 and geometry for the two types of solutions is not as great as in the Venus cases.

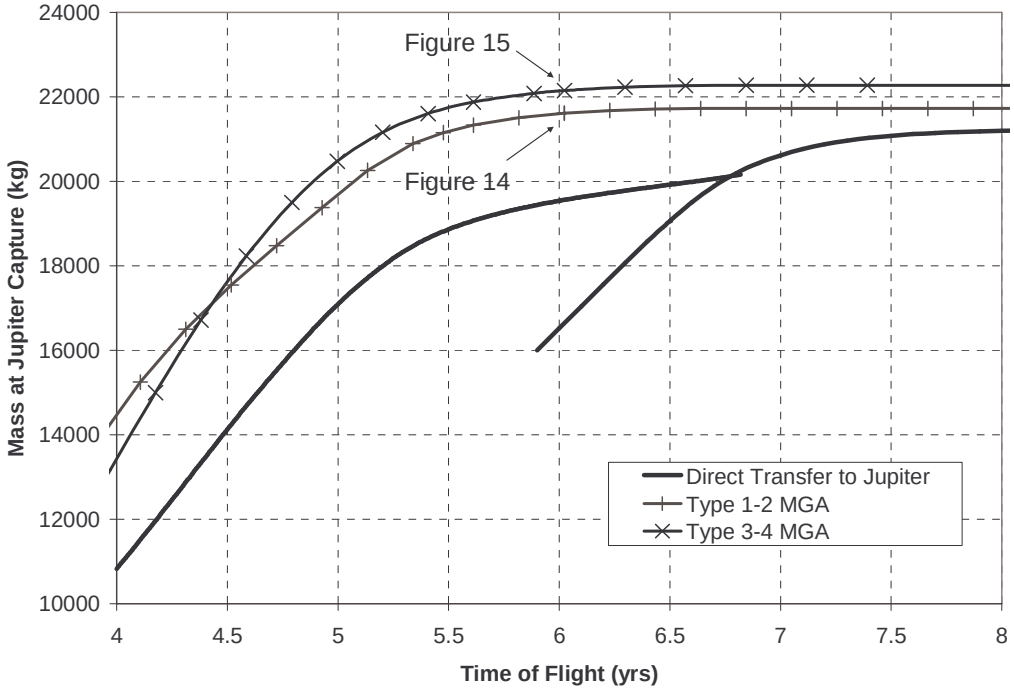

Figure 16 Mars Gravity Assists to Jupiter - Delivered Mass vs. Time of Flight

Both MGA trajectory types have phasing opportunities that occur roughly every two years. However, the two normally occur on different years so one opportunity of either type is likely to exist for any given launch year. Mars gravity assist performance varies substantially from opportunity to opportunity. For some injection opportunities the MGA performs worse than the VVGAs, though for most MGA opportunities this is not the case.

COMPARISON OF TRAJECTORY TYPES

Figure 17 shows the delivered mass vs. flight time curves for the two solution types of each of the three gravity-assist combinations along with the two direct trajectory types. All of the gravity-assist combinations offer an advantage at some time of flight over the direct cases. However, the Mars gravity assist offers the best delivered mass at most times of flight for these injection opportunities.

The direct Mars gravity-assist case outperforms the single VGA cases and the direct solutions for almost all times between 4 and 8 years. The Type 1-2 MGA outperforms the VVGA cases for flight times below 4.25 and above 6 years. However the Type 3-4 MGA outperforms all other investigated options at flight times above 5.25 years. Between 4.25 and 5.25 years the Type 1-2 VVGA case delivers the most mass. These relationships may change with different propulsion system characteristics or launch vehicle capability.

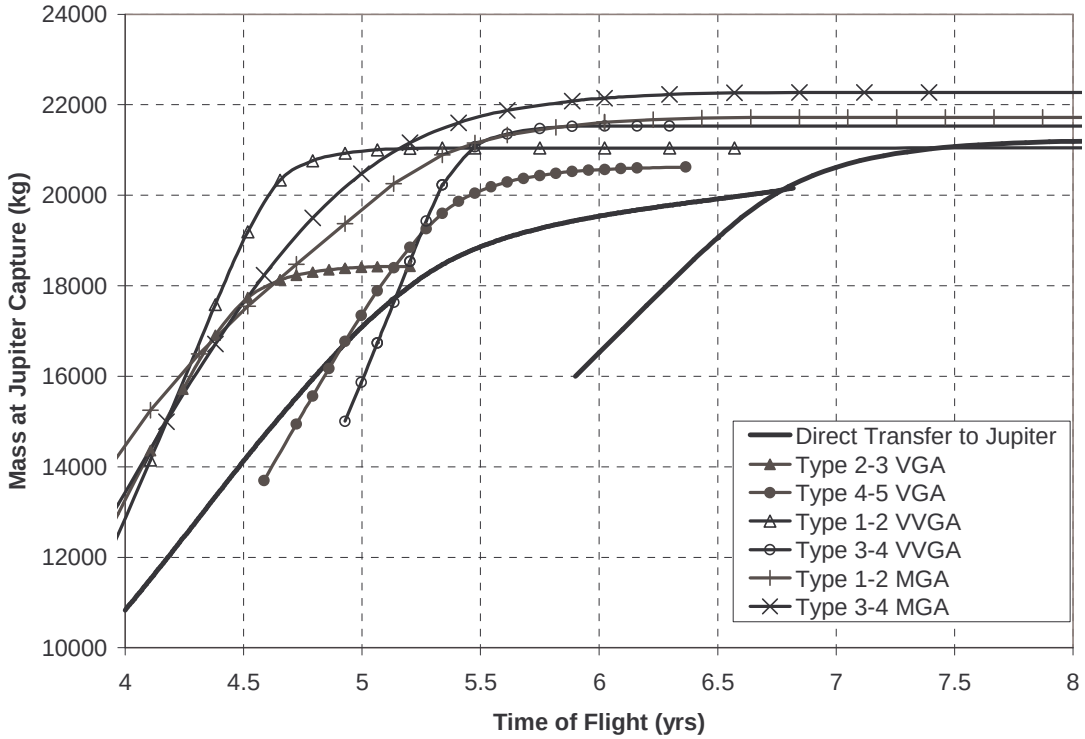

Figure 17 Gravity-Assist Combinations - Delivered Mass vs. Time of Flight

The Mars gravity assist has the advantage of having the lowest requirements for injection C_3 of all of the gravity-assist cases. The Type 1-2 VVGA offers more delivered mass than the Mars options at some flight times simply because it uses two gravity-assists at a much more massive planet that is closer to the sun. The double Venus option has an inherently larger minimum time of flight due to geometry than the Mars option, so one would expect Mars to offer more mass at very low flight times as shown in Figure 17. At longer flight times the Mars option benefits from a low injection C_3 and can outperform the other combinations.

A plot of low-thrust ΔV for the different gravity-assist options is shown in Figure 18. It is interesting to note that the MGA trajectories have a substantially higher ΔV than the VVGA trajectories while delivering comparable or greater masses to Jupiter due to the reduced C_3 at injection.

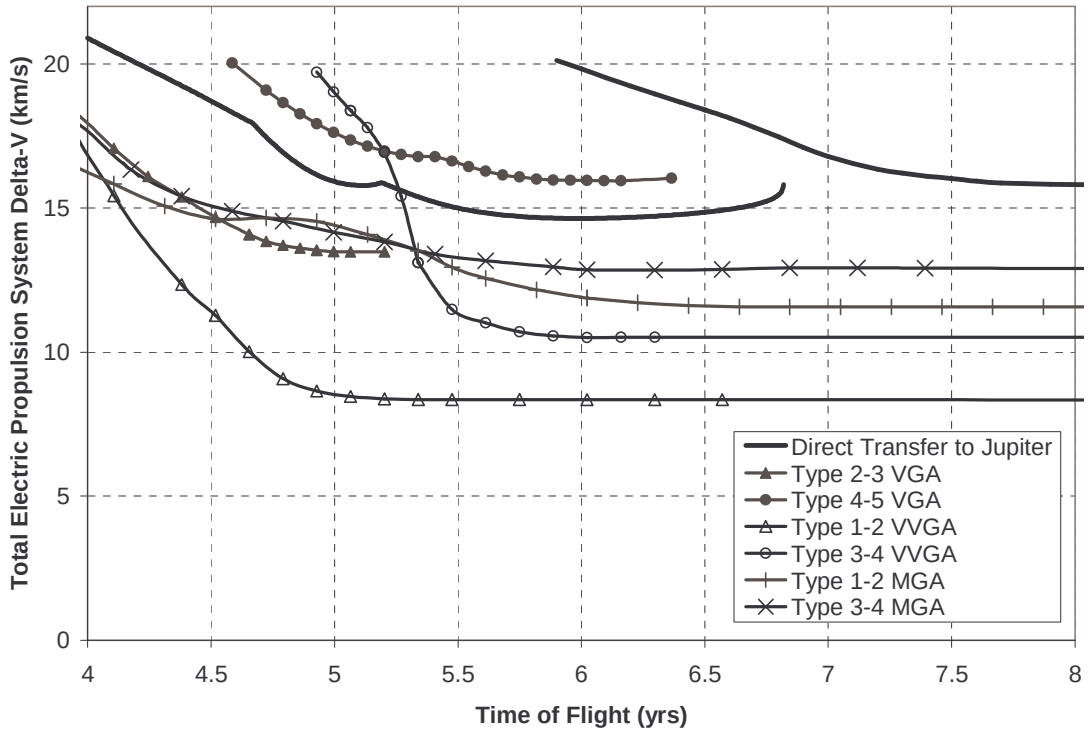

Figure 18 Gravity-Assist Combinations - ΔV vs. Time of Flight

It is also interesting to note that for each gravity-assist combination, the trajectories that require more heliocentric revolutions almost always require more ΔV than the corresponding gravity assist cases with fewer revolutions. This is due to the transfer of ΔV from the launch vehicle to the more efficient low-thrust system. Because of this effect, when comparing optimal C_3 trajectories, low-thrust ΔV alone cannot indicate which trajectories have the largest delivered mass to the target.

CONCLUSIONS

Many locally optimal solutions exist for low-thrust transfer trajectories. Solutions with multiple revolutions generally perform better at longer flight times. Trajectories with multiple heliocentric revolutions allow for a reduced initial injection C_3 and therefore increased initial mass allowing the more efficient ion engines to perform the necessary propulsion. The result is a significant increase in mass delivered to the target. In this way, low-thrust gravity-assist trajectories can benefit substantially from additional revolutions before the first flyby. However, trajectories with fewer numbers of heliocentric revolutions are the best options at low flight times.

The Type 3-4 MGA delivered the most final mass of the options studied at flight times higher than 5.25 years. At flight times between 4.25 and 5.25 years, the Type 1-2 VVGA offered the most final mass of the options considered. Below 4.25 years, the Type 1-2 MGA option delivers the most mass. Both of the single VGA cases and the Type 3-4 VVGA case underperformed at least one other option at all flight times examined.

The reduced initial C_3, and corresponding increased initial mass, of the trajectories with additional heliocentric revolutions result in increased low-thrust propellant consumption due to the reduction in energy supplied by the launch vehicle. The low-thrust ΔV for the gravity-assist options that traveled more

than 1 heliocentric revolution to the first encounter was higher than their counterparts with fewer revolutions for all of the gravity-assist combinations at most flight times.

ACKNOWLEDGEMENTS

The authors would like to thank Paul Finlayson and Ed Rinderle for their efforts in developing and enhancing the MALTO software and Anastassios Petropoulos for his helpful suggestions. This work was performed at the Jet Propulsion Laboratory, California Institute of Technology, under a contract with the National Aeronautics and Space Administration.

REFERENCES

[1] Williams, Steven N., and Coverstone-Carroll, Victoria, "Benefits of Solar Electric Propulsion for the Next Generation of Planetary Exploration Missions," *Journal of the Astronautical Sciences*, Vol. 45, No. 2, April-June 1997, pp. 143-159.

[2] Sauer, Carl G., Jr., and Yen, Chen-Wan L., "Planetary Mission Capability of Small Low Power Solar Electric Propulsion Systems," IAA-L-0706, IAA International Conference on Low-Cost Planetary Missions, Laurel, MD, April 12-15, 1994.

[3] Rayman, Marc D., and Lehman, David H. "NASA's First New Millennium Deep-Space Technology Validation Flight," IAA-L-0502, Second IAA International Conference on Low-Cost Planetary Missions, Laurel, MD, April 16-19, 1996.

[4] Debban, T. J., McConaghy, T. T., and Longuski, J. M., "Design and Optimization of Low-Thrust Gravity-Assist Trajectories to Selected Planets," AIAA/AAS Astrodynamics Specialists Conference, AIAA Paper 2002-4729, Monterey, CA, August 5-8, 2002.

[5] Maddock, R. W., and Sims, J. A., "Trajectory Options for Ice and Fire Preproject Missions Utilizing Solar Electric Propulsion," AIAA/AAS Astrodynamics Specialists Conference, AIAA Paper 98-4285, Boston, MA, August 10-12, 1998.

[6] Yam, C. H., McConaghy, T. T., Chen, K. J., and Longuski, J. M., "Preliminary Design of Nuclear Electric Propulsion Missions to the Outer Planets," AIAA/AAS Astrodynamics Specialist Conference, AIAA Paper 2004-5393, Providence, RI, August 16-19, 2004.

[7] Sims, J. A., and Flanagan, S. N., "Preliminary Design of Low-Thrust Interplanetary Missions," AAS/AIAA Astrodynamics Specialists Conference, AAS Paper 99-338, Girdwood, AK, August 16-19, 1999.

[8] Petropoulos, A.E., "Low-Thrust Orbit Transfers Using Candidate Lyapunov Functions with a Mechanism for Coasting," AAS/AIAA Astrodynamics Specialist Conference, AIAA Paper 2004-5089, Providence, RI, August 16-19, 2004.

[9] Sims, J. A., Longuski, J. M., and Staugler, A. J., "V_∞ Leveraging for Interplanetary Missions: Multiple-Revolution Orbit Techniques," *Journal of Guidance, Control, and Dynamics*, Vol. 20, No. 3, 1997, pp. 409-415.